FINAL TECHNICAL REPORT

FUNDAMENTAL PHYSICS AND PRACTICAL APPLICATIONS OF ELECTROMAGNETIC LOCAL FLOW CONTROL IN HIGH SPEED FLOWS

AIR FORCE OFFICE OF SCIENTIFIC RESEARCH
Grant No. FA9550-07-1-0246

Graham V. Candler

Department of Aerospace Engineering and Mechanics
University of Minnesota, Minneapolis MN 55455

candler@aem.umn.edu
612-625-2364 Fax: 612-626-1558

April 5, 2010

Report Documentation Page

Form Approved
OMB No. 0704-0188

1. REPORT DATE **05 APR 2010**	2. REPORT TYPE	3. DATES COVERED
4. TITLE AND SUBTITLE **Fundamental Physics and Practical Applications of Electromagnetic Flow Control in High Speed Flows**		5a. CONTRACT NUMBER 5b. GRANT NUMBER 5c. PROGRAM ELEMENT NUMBER
6. AUTHOR(S) **Graham Candler**		5d. PROJECT NUMBER 5e. TASK NUMBER 5f. WORK UNIT NUMBER
7. PERFORMING ORGANIZATION NAME(S) AND ADDRESS(ES) **University of Minnesota,110 Union Street SE,Minneapolis,MN,55455**		8. PERFORMING ORGANIZATION REPORT NUMBER
9. SPONSORING/MONITORING AGENCY NAME(S) AND ADDRESS(ES)		10. SPONSOR/MONITOR’S ACRONYM(S) 11. SPONSOR/MONITOR’S REPORT NUMBER(S)

12. DISTRIBUTION/AVAILABILITY STATEMENT
Approved for public release; distribution unlimited.

13. SUPPLEMENTARY NOTES

14. ABSTRACT
There are two overall objectives of the proposed research program. The first objective is to perform fundamental studies of microwave and combined microwave/laser energy deposition. The studies include characterization of the new microwave coaxial resonator at the University of Illinois, and development of kinetic-gasdynamic models for microwave and combined microwave/laser energy deposition in air. The second objective is to investigate practical applications of microwave and combined microwave/laser energy deposition for flow control in high speed flows relevant to the Air Force. These include control of 1) supersonic cavity flow 2) injection and mixing in a supersonic stream, 3) supersonic vehicle aerodynamics, and 4) Edney Type-IV shock interaction. This work studies the use of laser energy deposition to control mixing in a jet in supersonic crossflow. Detailed comparisons with new particle imaging velocimetry data from the University of Illinois are presented.

15. SUBJECT TERMS

16. SECURITY CLASSIFICATION OF:			17. LIMITATION OF ABSTRACT	18. NUMBER OF PAGES	19a. NAME OF RESPONSIBLE PERSON
a. REPORT **unclassified**	b. ABSTRACT **unclassified**	c. THIS PAGE **unclassified**		**16**	

Standard Form 298 (Rev. 8-98)
Prescribed by ANSI Std Z39-18

Abstract

The objective of the proposed research is the investigation of pulsed microwave and combined microwave/laser energy deposition for localized flow control in high speed (*i.e.*, supersonic and hypersonic) flows. The proposed effort is part of a developing broad research program in Electromagnetic Local Flow Control (ELFC). The main interest in ELFC is the need for fast response flow control systems for high speed aircraft. Conventional mechanical or electro-mechanical flow control devices have a typical response time which is several orders of magnitude too large for high speed aircraft. ELFC offers significant potential for a wide range of flow control devices and techniques with fast response times.

There are two overall objectives of the proposed research program. The first objective is to perform fundamental studies of microwave and combined microwave/laser energy deposition. The studies include characterization of the new microwave coaxial resonator at the University of Illinois, and developm ent of kinetic-gasdynamic models for microwave and combined microwave/laser energy deposition in air. The second objective is to investigate practical applications of microwave and combined microwave/laser energy deposition for flow control in high speed flows relevant to the Air Force. These include control of 1) supersonic cavity flow, 2) injection and mixing in a supersonic stream, 3) supersonic vehicle aerodynamics, and 4) Edney IV interaction.

The proposed research program is an extension of the current AFOSR-funded grant entitled "Fundamental Studies and Practical Applications of Electromagnetic Local Flow Control in High Speed Flows Using Laser Energy Deposition" (AFOSR Grant FA9550-04-1-0177, Jan 04 - Dec 06). Significant progress has been achieved in the current grant and is summarized in the proposal. Research progress in the fundamental studies include development of a kinetic model for microwave energy deposition in air, a kinetic-gasdynamic model for laser energy deposition in air, measurements of laser induced optical breakdown. Research progress in practical applications includes control of 1) terminal (normal) shock waves, 2) supersonic flow over a cavity, 3) Mach Reflection to Regular Reflection of crossing shock waves, 4) vortex breakdown in shock-vortex interaction, and 5) Edney IV interaction. In addition, two new facilities – a microwave energy deposition system and a supersonic wind tunnel – have been developed at the University of Illinois.

The proposed research program is a collaborative effort of Rutgers University, the University of Illinois at Urbana-Champaign and the University of Minnesota. In addition, the research includes a significant collaboration with the Institute for High Temperatures (Moscow, Russia) and St. Petersburg State University (St. Petersburg, Russia) who are separately funded by EOARD (London).

I. Introduction

To a large degree, the challenge of effective supersonic combustion is a problem of mixing. Aerothermodynamic concerns mandate a relatively short internal engine geometry, and efficient combustion requires fuel and air to be well mixed. A fuel injection scheme must possess the rather conflicting qualities of low internal drag and very rapid mixing. The problem is complicated by the fact that flight experiments are extremely expensive, and generation of reasonable freestream flow conditions in ground testing is very challenging. In addition, accurate measurement of a highly unsteady, high speed, intrinsically three-dimensions flow is difficult. For these reasons, there is great interest in numerical simulation of supersonic fuel injection. In order to develop confidence in these numerical studies, it is worthwhile to consider even very simple geometries. One of the most well-studied scenarios is the sonic transverse injection of fuel through holes flush with the combustor walls.

The gross flowfield that results from this normal injection is well understood and explained in the literature.[1−7] There are many cases of computational studies of this geometry. Traditionally, these have been Reynolds-Averaged Navier-Stokes (RANS) simulations that result in steady-state solutions. The works of Chenault *et al.*[8] and Sriram and Matthew[9] are characteristic of these steady-state nonreacting RANS simulations. These studies are very inexpensive and capture some important mean flow features, such as the shock structures and counter-rotating vortex pair (CVP) seen in Figure 1 taken from Reference 10. However, these steady simulations are quite unable to accurately simulate unsteady turbulent mixing. A more involved approach is needed to capture these effects.

A hybrid RANS and large-eddy simulation (LES) method can be constructed, based on the detached-eddy simulation (DES) formulation pioneered by Spalart *et al.*[11] The near-wall region in this approach is handled by the RANS portion of the method, which greatly reduces the computational cost compared to a LES resolved all the way to the wall. This wall-modeled large-eddy simulation (WMLES) approach allows routine computation of flows at Reynolds numbers beyond the reach of wall-resolved LES. This methodology has been previously applied to this class of problem. Srinivasan and Bowersox[12] simulated several non-reacting flows with the unmodified DES method. Boles *et al.*[13] investigated non-reacting injection with a hybrid RANS/LES method and compared their results with Mie scattering images. Kawai and Lele[14] investigated mixing mechanisms of a normal circular injector in a LES simulation. With further modifications of the DES methodology, Peterson and Candler[15] investigated several reacting flows with the circular normal injector.

In this report, we present results from a non-reacting modified DES simulation of the aforementioned geometry, run at flow conditions for which Lazar *et al.*[16] gathered particle image velocimetry (PIV) data. This comparison, an extension of our previous work, is done in order to further validate the effectiveness and accuracy of this methodology. The simulation compares both mean and root-mean-square (RMS) streamwise and wall-normal velocity fields on the centerline at a range of wall distances.

Lazar *et al.* also collected data on laser energy deposition, with the laser pulse located at the center of the jet outflow plane. High-speed photography allowed the tracking and investigation of the blast waves resulting from this energy deposition. We have endeavoured to duplicate this study of pulse blast wave dynamics. A straightforward and low-cost deposition technique has been implemented in our simulation software, using a simple local source term in the energy equation. This technique does not attempt to exactly model the physics within the volume of intense irradiance. However it is expected to accurately model the resultant hot region to the degree required for high-quality large-scale simulations. The implementation of the energy deposition has not yet been fully validated, and this effort continues as of this writing.

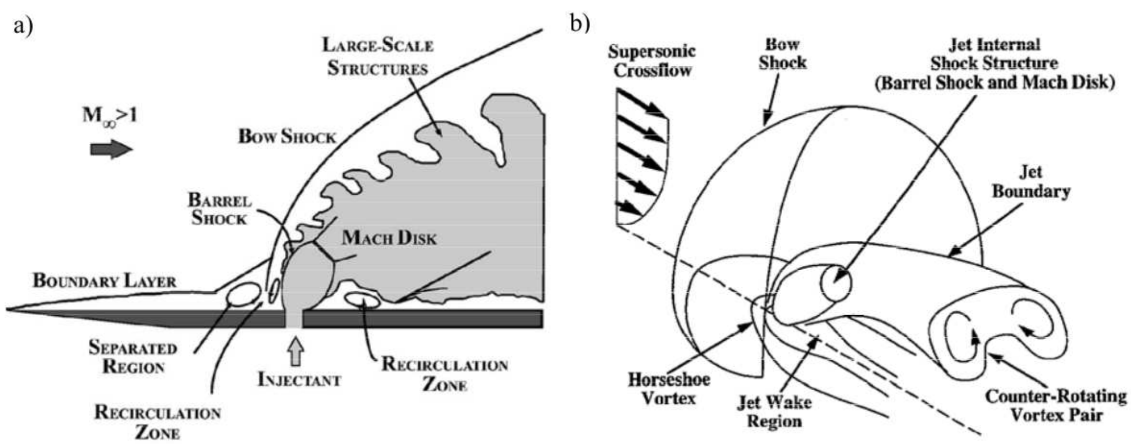

Figure 1. Illustration from Gruber *et al.*[10] of transverse injection into a supersonic crossflow: (a) instantaneous side view, (b) 3D view of average features.

II. Numerical Methods

The solver used in this study solves the compressible Navier-Stokes equations using a hybrid structured/unstructured, cell-centered finite volume approach.[17] The inviscid fluxes can be evaluated using a low dissipation version of the Steger-Warming method with either a second-order or third-order, upwind-biased reconstruction. A recently developed low-dissipation flux evaluation method which is kinetic energy conserving has also been incorporated into the flow solver. Smooth regions of the flow are handled by this low-dissipation scheme; in regions of strong gradients, the flux evaluation reverts to Steger-

Warming. The gradients in the viscous terms are calculated using weighted least-squares fits.

Time integration within the solver is currently formally first-order accurate. The parallel Full-Matrix Point-Relaxation method (FMPR)[18] is used for time integration. The FMPR method is fully implicit and is not subject to the impractical time step limitation of explicit methods.

The unstructured approach and implicit time integration are enabling features for simulating the type of complex flows of interest in this report. The unstructured methodology allows for key flow features to be well resolved without the penalty of carrying that resolution to other parts of the domain where it is unnecessary. That is, the grids can be made to make every cell count. Implicit time integration allows for time steps to be taken which are large enough that meaningful amounts of physical time can be simulated in reasonable amounts of computer run time.

A. Turbulence Modeling

The simulation presented uses a wall-modeled large-eddy simulation (WMLES) approach to turbulence closure, with Reynolds-Averaged Navier-Stokes (RANS) providing the wall closure. The switch between wall-modeled RANS regions and LES regions is handled by a formulation developed by Travin *et al.*[19] The particular approach used for the simulation is an Improved Delayed Detached-Eddy Simulation (IDDES) formulated by the same group and presented by Shur *et al.*[20] The one-equation turbulence model of Spalart and Allmaras,[21] with density corrections of Catris and Aupoix,[22] is used as the baseline RANS model. The DES constant used is the standard value of 0.65. This IDDES formulation with the aforementioned single-equation model shall henceforth be referred to as the hybrid-SA model.

In the interest of brevity, full details of the hybrid method will not be repeated here; the interested reader is referred to the discussion by Travin *et al.*[19] However, several items are of note. DES97 suffers from the limitation that the LES-RANS switch is solely a function of the grid, and so applies LES methodology in attached regions where no turbulence is present. The switch used in IDDES is a function of the solution itself, so that RANS behavior is maintained in regions where no LES content is present. The IDDES method also redefines the subgrid length scale near the wall, addressing the 'log-layer mismatch' WMLES issue identified by Nikitin et al.[23]

B. Inflow Conditions

The configuration of the wind tunnel nozzle used in the experiment is known, allowing the aforementioned upsteam RANS calculation to generate the proper boundary layer thickness. The freestream stagnation pressure in the experiment was 279 kPa and the stagnation temperature 300 K; these values were used in the upstream calculation. The stagnation pressure of the injectant was 378 kPa, and the stagnation temperature was also 300 K. The injector diameter was 4.8 mm. Both the injectant and the bulk flow were air. The simulation was performed as a two-species calculation with both species identical.

C. Grid Generation and Boundary Conditions

The grid used for this simulation is composed of unstructured hexahedral cells (Figure 2). It was created using the commercial grid generation software GridPro, which is amenable to sophisticated topology-based local refinement. This allows the dense clustering of cells in the region of the jet plume, smoothly and rapidly decreasing in resolution in three dimensions, without resulting in regions of locally high anisotropy. The computational domain extends 10 injector diameters out from the wall, 10 diameters to each side, 5 diameters upstream and 15 diameters downstream. The grid is clustered to the wall such that the first cell was within one wall unit. The final grid contains 10,760,218 hexahedral elements.

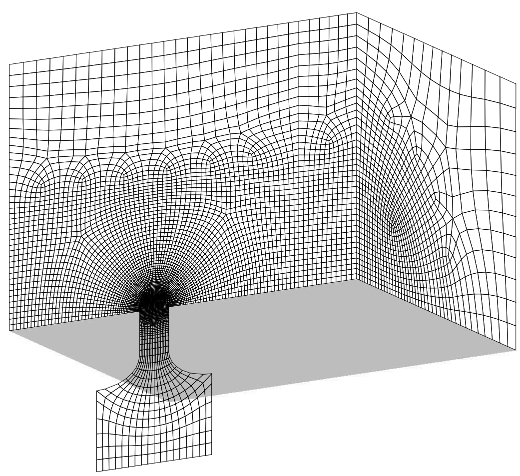

Figure 2. Example of nested-refinement grid. Note that grid is shown with substantial global de-refinement for clarity

The wall containing the injector, and the injector walls and plenum, are adiabatic no-slip walls with a temperature of 300 K. The plenum contains a subsonic injection boundary condition, in which the solver adjusts pressure in order to satisfy a specified mass flow rate and total temperature. The far-field walls are outflow conditions, as the region of interest is far from the walls and showed no reflected shocks in the experimental results.

III. Results and Discussion

Simulations were run on 256 cores of a quad-core AMD Opteron cluster. The time step was chosen such that the local CFL number (CFL number is the non-dimensionalized time step based on the grid spacing and the maximum characteristic flow speed) for cells within the jet plume was less than unity. At the chosen time step, approximately 174 iterations are required to computer one flow time (based on the jet exit diameter and the freestream velocity). A single iteration requires approximately 3.1 seconds with the number of cores used, so that 160 flow times can be computed in a 24 hour period.

The simulation was initialized in conventional RANS mode, with conventional flux evaluation and large time steps, in order to quickly establish the injector mass flow and to allow undesired numerical-startup transients to flow out of the domain. This flow was allowed to proceed for 160 flow times (which, at these much larger timesteps, was completed in a few hours) in order to ensure that the injector mass flow had reached steady state. The simulation was then restarted in DES97 mode, and the low-dissipation flux evaluation activated. This intermediate step is necessary due to the nature of the hybrid-SA model, which will not switch regions to LES if they do not already possess LES content. Of course, there is zero LES content in pure RANS results. The intermediate DES97 iterations seed the domain with LES content in the appropriate regions. This DES97 simulation was run for 5000 iterations, or about 29 flowtimes. The simulation was once more restarted, but this time in full hybrid-SA mode. The simulation was then run for 50 flowtimes to ensure that all restart-related transients have disappeared, and the simulation was run for 300 flowtimes to completion. Statistical data were generated during these last 300 flow times, and it is these data that are compared to experiment.

A. Mean Velocity Field

Figure 3 shows two time-averaged streamwise velocity fields, one from experiment and one from simulation. The experimental images are ensemble averages of 640 PIV images; the simulated velocity field is averaged over 300 flow times. Both plots show some of the characteristic flow details represented in Figure 1, although the upstream edge of the barrel shock does not stand out. There is only slight disagreement in velocity magnitude in the region aft of the barrel shock. Note that the PIV data do not extend precisely to the wall; the method is not amenable to measurements arbitrarily close to a solid boundary.

Figure 4 compares the wall-normal velocity fields, averaged as previously. Here, the barrel shock and Mach disk are immediately apparent. It appears that the downstream recirculation region may be further downstream in the simulation, but the lack of near-wall PIV data does not allow a concrete conclusion.

Overall, agreement between experiment and simulation is very good. The simulation is accurately capturing all of the flow physics that can be resolved by the PIV data from experiment. All of the steady-state centerline flow features identified in the literature, and shown in Figure 1, are clearly visible.

B. RMS Velocity Field

In many respects, the RMS plots reinforce the observations derived from the mean velocity fields. Apparent in Figure 5 is the difference in streamwise RMS velocity just downstream of and below the barrel shock. The reason for this disparity is not immediately clear, but it should be remembered that both experimental and simulation data are, by necessity, spatial and temporal averages. As such, small differences in size and location of time-variant flow feature data does not necessarily indicate disparity in the actual flow. The rest of the flowfield is in very good agreement. As previously mentioned, the large-area variation very near the wall is not necessarily noteworthy. The areas of large RMS velocities appear to be somewhat further from the wall in the simulation, but the near-wall limitations of PIV must be kept in mind.

Figure 6 does not exhibit any regions of substantial disagreement. The region downstream of the barrel shock is different in detail but similar in general (especially keeping in mind the space/time averaging issue). Again, regions of high RMS velocities appear to be further from the wall in the simulation compared to the experiment, particularly the high-valued red 'tail' trailing from below the Mach disk. The simulation also presents a larger volume of moderate-valued RMS velocity above the aforementioned 'tail', although in both plots there is a distinct lower-valued region emanating from the Mach disk itself. In general, the experimental and numerical data are in good agreement.

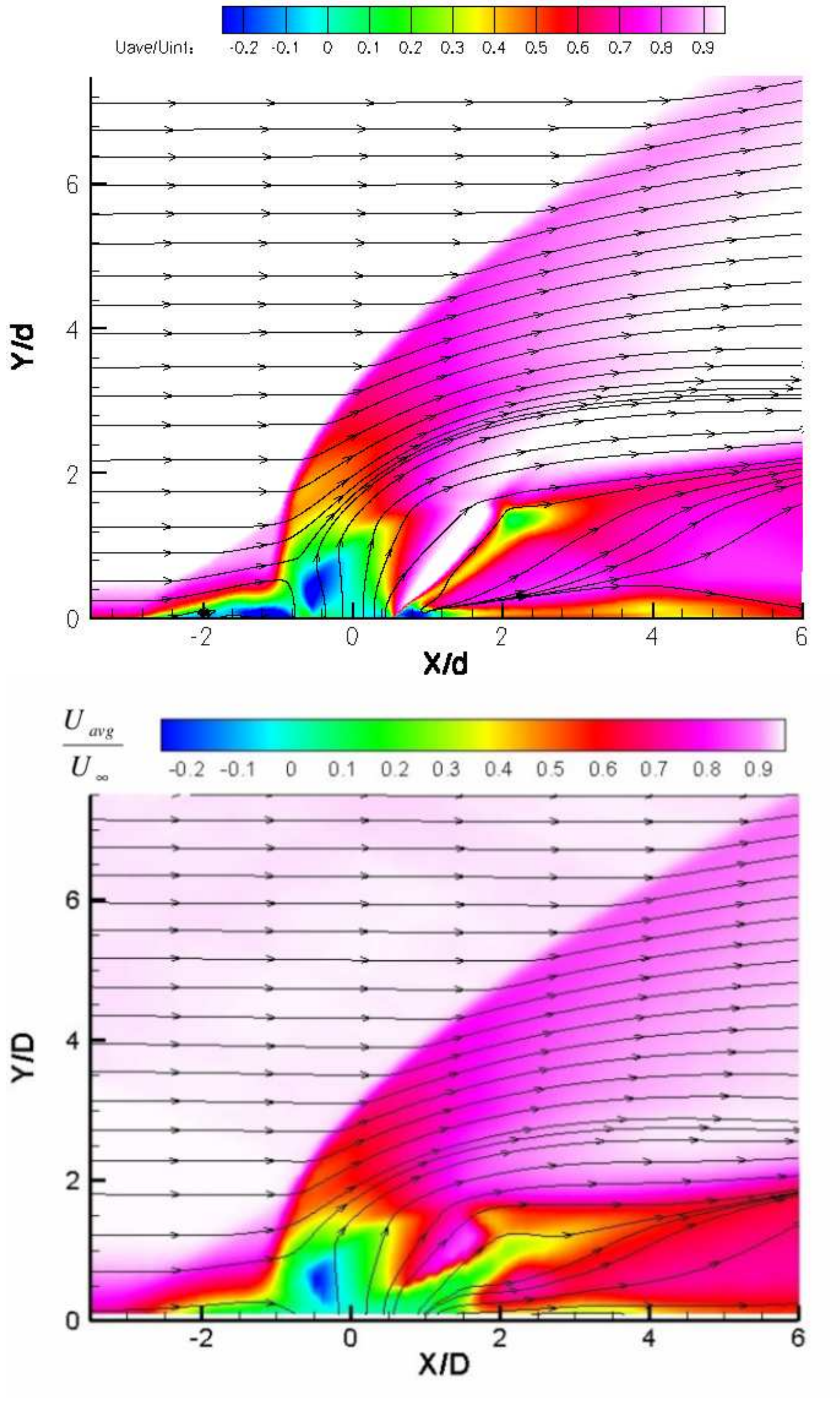

Figure 3. Contours of normalized mean streamwise velocity. Simulation upper, experiment[16] lower.

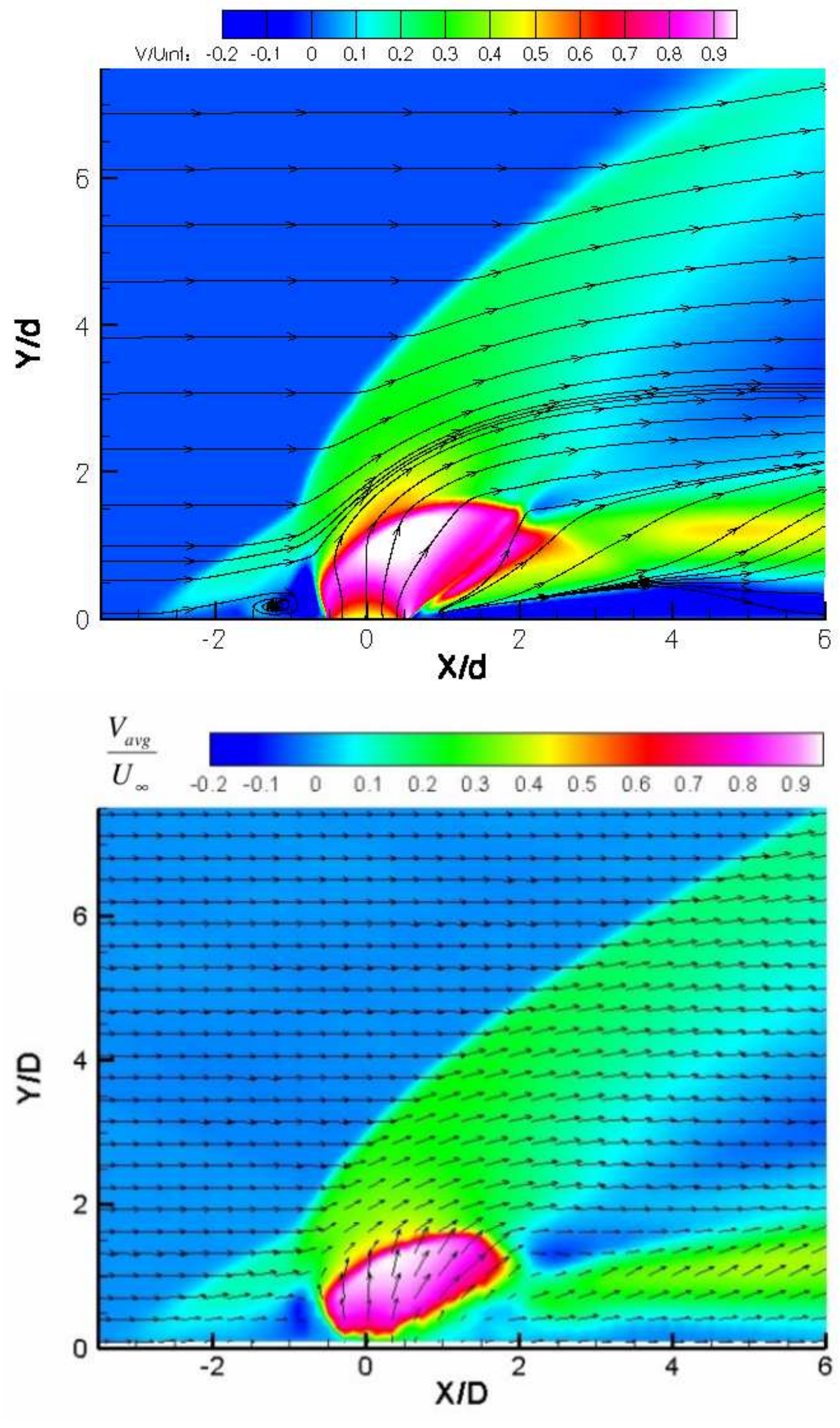

Figure 4. Contours of normalized mean wall-normal velocity. Simulation upper, experiment[16] lower.

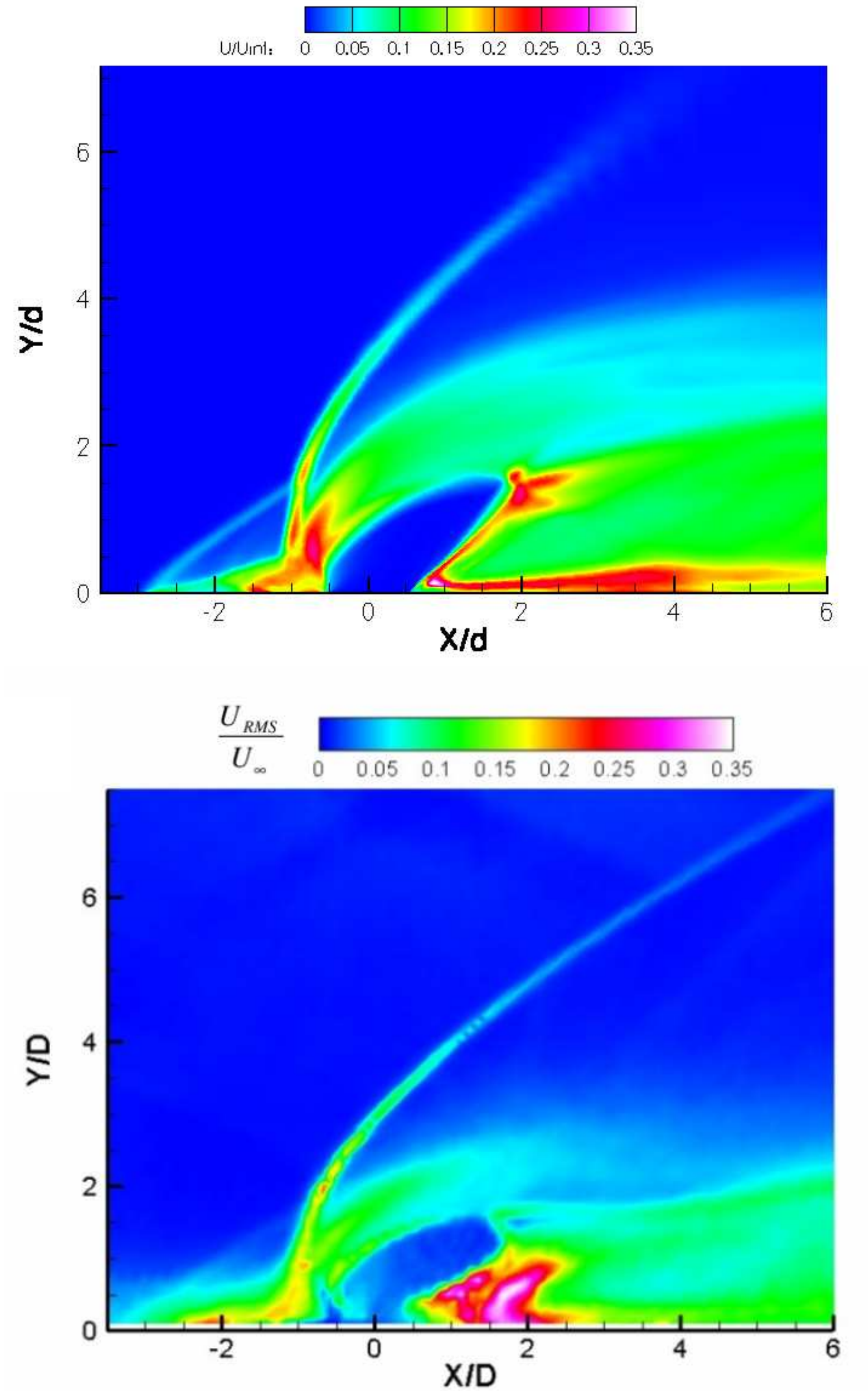

Figure 5. Contours of normalized RMS streamwise velocity. Simulation upper, experiment[16] lower.

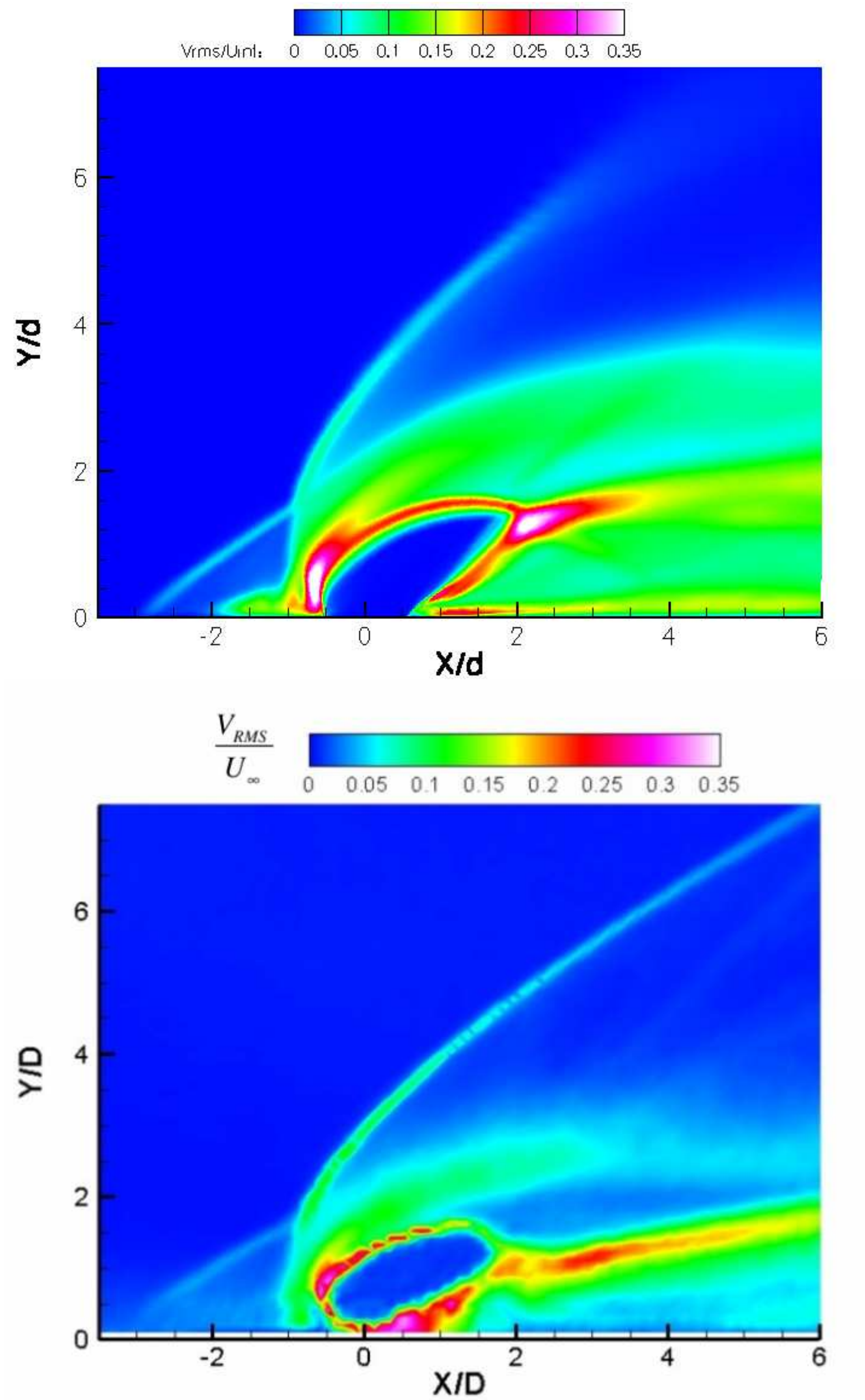

Figure 6. Contours of normalized RMS wall-normal velocity. Simulation upper, experiment[16] lower.

Simulations are, by nature, quite amenable to complex visualization of volume flow features. Figure 7 shows an instantaneous plot of the vortical structures in the flow (demarcated by the Q-criterion, the second principle invariant of the velocity gradient tensor). The slices shown are temperature contours. Here, the flow features of Figure 1 are extremely clear. Notable is the wide range of length scales resolved by the simulation; capturing this range of scales is absolutely critical to the accurate simulation of mixing. Especially prominent is the strong and well-defined horseshoe vortex eminating from the upstream separation region. Also of interest is the fact that the inflow was not "seeded"[24,25] with any small-scale fluctuations: the highly complex upstream separation region is completely a function of the strong shock nearby. The low-dissipation numerics detailed above are an enabling technology for simulation of these structures. The physical generation and long lifespan of these small structures could not be captured with other schemes without an infeasably large grid.

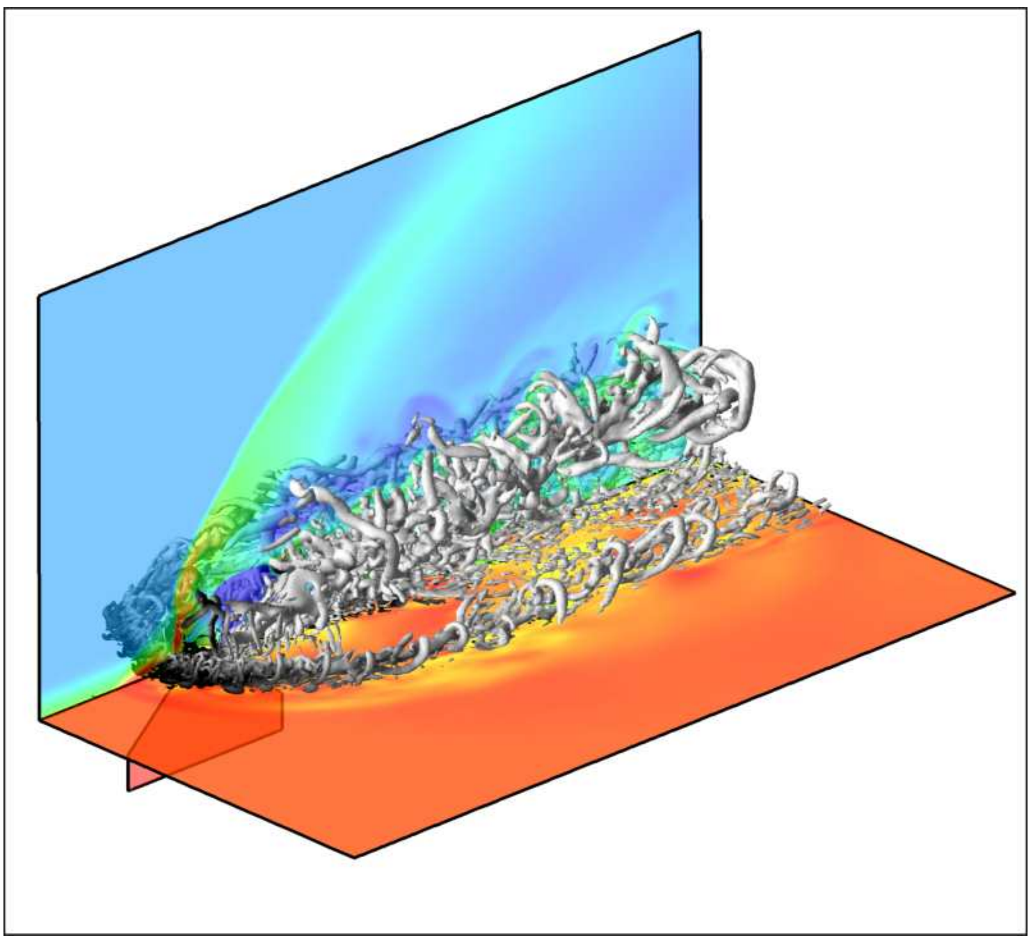

Figure 7. Isosurfaces of Q-criterion; temperature contours.

IV. Conclusions

Simulations of air injection into a supersonic crossflow were performed using a hybrid RANS / LES methodology based on the detached-eddy simulation method, including a low-dissipation flux evaluation scheme that captures a large range of length scales. This methodology allows for relatively inexpensive simulation of large-scale unsteady flow structures in these supersonic-combustor-like geometries. Results from these simulations have been compared to experiment. The mean velocities of the simulated flow were found to closely match the mean velocities from experiment. The RMS velocities exhibited some minor discrepancies but were very similar overall. Visualization of the entire volume of the flow shows all of the flow features understood to exist in these crossflow injectors. Laser energy deposition was performed in experiments. Numerical techniques for this energy deposition have been developed and included in the flow solver, but the implementation has not yet been fully validated and applied to this case.

V. Future Work

The proposed research was to take accurate simulations of a jet in crossflow as shown above, and add pulsed energy deposition to model a laser spark. The laser energy deposition local, energy, and frequency were to be varied to see if enhanced mixing would occur with this means of flow control. There have been a number of problems that have prevented us from completing this study. First, the experimental data were very slow to be produced, there were important discrepancies between simulation and experiment that had to be understood and solved, and the laser energy deposition model had to be reconstituted and coded into a different computational fluid dynamics code. At this point, all of these problems have been worked out and we are now beginning to produce meaningful results with laser energy deposition for this problem. The results of this work will be presented at the forthcoming 40$^{\text{th}}$ Americal Institute of Aeronautics and Astronautics (AIAA) Fluid Dynamics conference.[26] The accompanying paper will have full details of this study.

Acknowledgments

The authors would like to thank Eli Lazar, Dr. Gregory Elliott, and Dr. Nick Glumac of the University of Illinois at Urbana-Champaign for providing data from their experimental studies. This work was sponsored by the Air Force Office of Scientific Research under grant FA9550-07-1-0246. The views and conclusions contained herein are those of the author and should not be interpreted as necessarily representing the official policies or endorsements, either expressed or implied, of the AFOSR or the U.S. Government.

References

1. Schetz, J.A., and Billig, F.S., "Penetration of Gaseous Jets Injected into a Supersonic Stream," *Journal of Spacecraft and Rockets,* Vol. 3, No. 11, 1966, pp. 1658-1665.

2. Schetz, J.A., Hawkins, P.F., and Lehman, H., "Structure of Highly Underexpanded Transverse Jets in a Supersonic Stream," *AIAA Journal,* Vol. 5, No. 5, 1967, pp. 882-884.

3. Papamoschou, D., Hubbard, D.G., and Lin, M., "Observations of Supersonic Transverse Jets," AIAA Paper No. 91-1723, June 1991.

4. Hermanson, J.C., and Winter, M., "Mie Scattering Imaging of a Transverse, Sonic Jet in Supersonic Flow," *AIAA Journal,* Vol. 31 No. 1, 1993, pp. 129-132.

5. Santiago, J.G., and Dutton, J.C., "Velocity Measurements of a Jet Injected into a Supersonic Crossflow," *Journal of Propulsion and Power,* Vol. 13 No. 2, 1997, pp. 264-273.

6. Everett, D.E., Woodmansee, M.A., Dutton, J.C., and Morris, M.J., "Wall Pressure Measurements for a Sonic Jet Injected Transversely into a Supersonic Crossflow," *Journal of Propulsion and Power,* Vol. 14 No. 6, 1998, pp. 861-868.

7. VanLerberghe, W.M., Santiago, J.G., Dutton, J.C., and Lucht, R.P., "Mixing of a Sonic Transverse Jet Injected into a Supersonic Flow," *AIAA Journal,* Vol. 38 No. 3, 2000, pp. 470-479.

8. Chenault, C.F., Beran, P. S., and Bowersox, R. D. W., "Numerical Investigation of Supersonic Injection Using a Reynolds-Stress Turbulence Model," *AIAA Journal,* Vol. 37, No. 10, Oct..1999, pp. 1257-1269.

9. Sriram, A.T., and Matthew, J., "Numerical Simulation of Transverse Injection of Circular Jets into Turbulent Supersonic Streams," *Journal of Propulsion and Power,* Vol. 24, No. 1, 2008.

10. Gruber, M. R., Nejad, A. S., Chen, T. H., and Dutton, J. C., "Mixing and Penetration Studies of Sonic Jets in a Mach 2 Freestream," *Journal of Propulsion and Power,* Vol. 11, No. 2, 1995, pp. 315-323.

11. Spalart, P. R., Jou, W-H., Strelets, M., and Allmaras, S. R., "Comments on the Feasibility of LES for Wings and on a Hybrid RANS/LES Approach," Advances in DNS/LES, 1st AFOSR International Conference on DNS/LES, August 4-8, 1997, Greyden Press, Columbus, OH.

12. Srinivasan, R., and Bowersox, R.D.W., "Assessment of RANS and DES Turbulence Models for Supersonic Jet Interaction Flows," AIAA Paper No. 2005-499, Jan. 2005.

13. Boles, J., and Edwards, J., "Hybrid LES/RANS Simulation of Normal Injection into a Supersonic Cross-Stream," AIAA Paper No. 2008-622, Jan. 2008.

14. Kawai, S. and Lele, S.K., “Mechanisms of Jet Mixing in a Supersonic Crossflow: A Study Using Large-Eddy Simulation,” AIAA Paper No. 2008-4575, July 2008.

15. Peterson, D.M., and Candler, G.V., “Hybrid RANS/LES of a Supersonic Combustor,” AIAA Paper No. 2008-6923, Aug. 2008.

16. Lazar, E., Elliott, G., and Glumac, N., “Energy Deposition Applied to a Transverse Jet in a Supersonic Crossflow,” AIAA Paper No. 2009-1534, Jan. 2009.

17. Nompelis, I., Drayna, T.W., and Candler G.V., “Development of a Hybrid Unstructured Implicit Solver for the Simulation of Reacting Flows Over Complex Geometries,” AIAA Paper No. 2004-2227, June 2004.

18. Wright, M.J., Candler, G.V., and Prampolini, M., “Data-Parallel Lower Upper Relaxation Method for the Navier-Stokes Equations,” *AIAA Journal,* Vol. 34, No. 7, 1996, pp. 1371-1377.

19. Travin, A.K., Shur, M.L., Spalart, P.R., and Strelets, M.K., “Improvement of Delayed Detached-Eddy Simulation for LES with Wall Modelling,” ECCOMAS CFD, 2006.

20. Shur, M.L., Spalart, P.R, Strelets, M.K., and Travin, A.K., “A hybrid RANS-LES approach with delayed-DES and wall-modelled LES capabilities,” *International Journal of Heat and Fluid Flow,* Vol. 29, No. 6, Dec. 2008, pp. 1638-1649.

21. Spalart, P. R., and Allmaras, S.R., “A One-Equation Turbulence Model For Aerodynamic Flows,” AIAA Paper No. 1992-0439, 1992.

22. Catris, S., and Aupoix, B., “Density Corrections for Turbulence Models,” *Aerosp. Sci. Technol.,* Vol. 4, 2001.

23. Nikitin, N.V., Nicoud, F., Wasistho, B., Squires, K.D., Spalart, P.R., “An Approach to Wall Modeling in Large-Eddy Simulations,” *Phys. Fluids,* Vol. 12, No. 7, 2000.

24. Peterson, D.M., Subbareddy, P.K., and Candler, G.V. “Assessment of Synthetic Inflow Generation for Simulating Injection Into a Supersonic Crossflow,” AIAA Paper No. 2006-8128, Nov. 2006.

25. Subbareddy, P.K., Peterson, D., Candler, G. V., and Marusic, I., A Synthetic Inflow Generation Method Using the Attached Eddy Hypothesis,” AIAA Paper No. 2006-3672, June 2006.

26. Tylczak, E., Peterson, D., and Candler, G.V., “Hybrid RANS/LES Simulation of Transverse Jet in Supersonic Crossflow,” AIAA-2010-4856, June 2010.